

Growth of Interfacial Cracks in Sandwich Beams

E.E. Gdoutos* and V. Balopoulos

School of Engineering, Democritus University of Thrace, GR-671 00 Xanthi, Greece

Abstract: Debonding between core and facings is a common failure mode of sandwich structures that can severely damage the load-carrying capacity of the structure. The objective of this work is to study the effect of debonding in double cantilever beam specimens made of aluminum facings and PVC foam cores. The configuration follows the standard ASTM D5528-94a peel test. Four PVC foam core materials under the commercial name Divinycell H with densities 60, 80, 100, and 250 kg/m³ are considered. In each case debonding is introduced between the core and the adhesive at the loaded facing of the beam. Linear elastic fracture mechanics is used to model interfacial crack growth and crack kinking into the core. Due to the different mechanical properties of the adjoining materials mixed-mode loading conditions dominate in the neighborhood of the crack tip. Results for the stress and displacement fields are obtained using a finite element computer code. The energy release rate and both opening- and sliding-mode stress intensity factors for interfacial and core cracks are calculated and found that they can be approximated as linear functions of crack length. From results of stress intensity factors in conjunction with the maximum circumferential stress criterion it was obtained that for weak interfaces debonding grows along the interface. On the contrary, for strong interfaces, crack kinks into the core, followed by rapid curving. After a small initial curved depth h_{∞} the crack becomes parallel to the interface. It was obtained that h_{∞} is inversely proportional to the modulus of elasticity of the core material and independent of the core thickness.

Keywords: Sandwich beams, Debonding, Foam cores, Finite elements, Linear elastic fracture mechanics, Strain energy release rate.

1. INTRODUCTION

Sandwich structures are composed of dissimilar materials and exhibit various failure modes including facing compression or tension failure, core shear failure, compression facing wrinkling, indentation failure and debonding between the core and the facings. Failure modes can be caused by accidental overloads of the structure or by initial defects. Sandwich structures offer improved stiffness and strength to weight ratios compared to monolithic materials. Furthermore, they present excellent thermal and acoustic insulation properties. They have found wide applications in weight-sensitive structures where the main loads are flexural.

A thorough investigation of failure modes of composite sandwich structures made of carbon/epoxy facings and PVC foam core materials was performed by Daniel and Gdoutos [1-5]. Debonding between core and facings is a serious failure mode of sandwich structures. It can be modeled as an interface crack between dissimilar materials and studied by linear elastic fracture mechanics (LEFM) [6, 7]. Zenkert [8] applied LEFM to analyze the facings to core debonding in sandwich structures. Carlsson and Prasad [9-11] studied the mixed-mode fracture in a sandwich plate for different loadings on the debonding sandwich facing. A comprehensive study of the facing to core debonding was performed by Ratcliffe and Cantwell [12]. Østergaard *et al.* [13] measured the interface toughness in sandwich double cantilever beams

made of glass/polyester facings and PVC cores and found that it strongly depends on the mode mixity. Berggreen *et al.* [14] developed a numerical model based on finite elements for the prediction of debonding between facing and core in foam core sandwich structures. Grau *et al.* [15] determined the interfacial fracture toughness in composite sandwich panels made of graphite/epoxy facings and an aramid fiber/phenolic resin honeycomb core. They found that the interfacial fracture toughness increases as much as 70% as the shear component increases, which leads to an overestimation of the load carrying capacity of debonded sandwich panels.

In the present work we consider a sandwich double cantilever beam (DCB) specimen made of aluminum facing and foam core with initial debonding in the form of an interfacial crack (Fig. 1). The growth behavior of the interfacial crack is studied by a finite element analysis coupled with failure criteria. The fundamentals of interfacial crack propagation in linear elastic fracture mechanics (LEFM) are first presented. Then, we describe the materials and the geometry of the sandwich DCB specimen and its discretization. From the finite element analysis we obtain results for the strain energy release rate and the opening- and sliding-mode stress intensity factors for the interfacial crack. These results are coupled with the maximum circumferential stress criterion [16] to obtain the crack growth behavior in the core. Results for the dependence of the crack growth path in the core are obtained as a function of the stiffness of the core. It was found that for weak interfaces debonding grows along the interface, while for strong interfaces crack kinks into the core, followed by rapid curving. After a small initial curved depth h_{∞} the crack becomes parallel to the interface. It was obtained

*Address correspondence to this author at the School of Engineering, Democritus University of Thrace, GR-671 00 Xanthi, Greece; Tel: +30-25410-796; Fax: +30-25410-79652; E-mail: egdoutos@civil.duth.gr

that h_∞ is inversely proportional to the modulus of elasticity of the core material and independent of the core thickness.

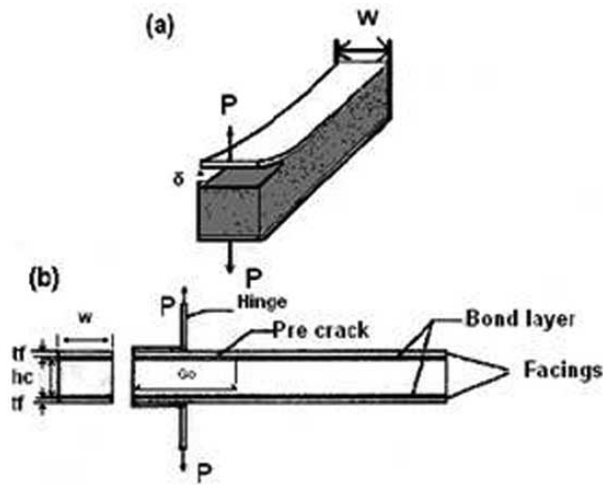


Fig. (1). Sandwich peel test specimen.

2. INTERFACIAL CRACKS

In this section we provide a theoretical background of the mechanics of fracture of cracks along bimaterial interfaces. It will help the reader to understand the problems encountered in dealing with interfacial cracks in the rest of the paper.

Consider an interfacial crack between two dissimilar materials, 1 and 2 (Fig. 2). We briefly present the fundamentals of fracture mechanics of interfacial cracks [17-20]. In elastic problems of bimaterial bodies two parameters α and β ($j \in \{1,2\}$), that express the mismatch of the elastic properties of the adjoining materials, are defined by [21]:

$$\left. \begin{aligned} \alpha &= \frac{\bar{E}_1 - \bar{E}_2}{\bar{E}_1 + \bar{E}_2} \\ \beta &= \frac{G_1(\kappa_2 - 1) - G_2(\kappa_1 - 1)}{G_1(\kappa_2 + 1) + G_2(\kappa_1 + 1)} \end{aligned} \right\}, \text{ where } G_j = E_j/2(1+\nu_j) \text{ and} \quad (1)$$

$$\left\{ \begin{aligned} \bar{E}_j &= E_j/(1-\nu_j^2), \quad \kappa_j = 3-4\nu_j \text{ for plane strain} \\ \bar{E}_j &= E_j, \quad \kappa_j = (3-\nu_j)/(1+\nu_j) \text{ for plane stress} \end{aligned} \right.$$

The singular normal and shear stresses, σ_{yy} and τ_{xy} , and the opening and sliding displacements of the crack faces δ_x and δ_y , along the crack axis are given by [7]:

$$\sigma_y + i\tau_{xy} = \frac{K r^{i\epsilon}}{\sqrt{2\pi r}} \quad \text{and} \quad \delta_y + i\delta_x = \frac{4(1/\bar{E}_1 + 1/\bar{E}_2)}{(1+2i\epsilon) \cosh(\pi\epsilon)} \sqrt{\frac{r}{2\pi}} K r^{i\epsilon}, \quad (2)$$

where $K = K_1 + iK_2$ and $\epsilon = \frac{1}{2\pi} \ln\left(\frac{1-\beta}{1+\beta}\right)$

In the above equation K is the complex stress intensity factor and K_1 and K_2 are the opening-mode and sliding-mode stress intensity factors. Note that the displacement field has an oscillatory term $r^{i\epsilon}$ which leads to overlapping of the crack faces in a very small area near the crack tip. For most practical applications β is small and it can be assumed equal

to zero. Under such circumstances no overlapping of the crack faces takes place.

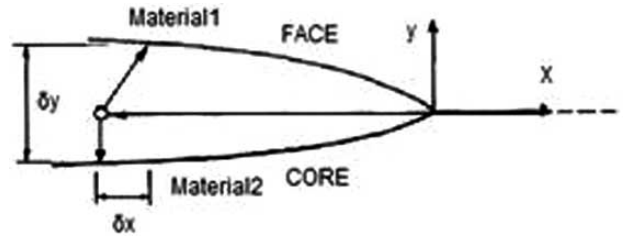


Fig. (2). Interfacial crack between two dissimilar materials.

Thus, the singular stress and displacement fields in the neighborhood of the interfacial crack are proportional to [7]

$$\{\sigma_y, \tau_{xy}\} = \frac{\{K_I, K_{II}\}}{\sqrt{2\pi r}} \quad \text{and} \quad \{\delta_y, \delta_x\} = \frac{4(1/\bar{E}_1 + 1/\bar{E}_2)\sqrt{r}}{\sqrt{2\pi}} \{K_I, K_{II}\} \quad (3)$$

The strain energy density is given by [7]

$$G_{int} = \frac{1}{2} \left[\frac{1}{E_1} + \frac{1}{E_2} \right] (K_I^2 + K_{II}^2) \quad (4)$$

For similar materials ($\bar{E}_1 = \bar{E}_2 = \bar{E}$) Eq. (4) gives the value of the strain energy release rate for a crack in a monolithic elastic material as:

$$G_{vol} = \frac{K_I^2 + K_{II}^2}{\bar{E}} \quad (5)$$

The interfacial crack may propagate along the interface or kink into one of the adjoining materials. The angle of initial crack propagation, Ω , is given, according to the maximum tangential (hoop) stress criterion [16], by:

$$\Omega = 2 \tan^{-1} \left(\frac{\sqrt{1 + 8(K_{II}/K_I)^2} - 1}{4K_{II}/K_I} \right) \quad (6)$$

Kinking of the interfacial crack into the core occurs when the following inequality is satisfied:

$$\left(\frac{\max G}{G_{l,cr}} \right)_{core} > \left(\frac{G}{G_{cr}(\gamma)} \right)_{int} \quad (7)$$

The critical strain energy release rate for the core material in mode I, $G_{l,cr}$, and the critical interfacial strain energy release rate, $G_{cr}(\gamma)$, as function of mode mixity, are determined experimentally. They are characteristic parameters of the core and the interface, respectively. On the other hand, the values of energy release rate for crack growth in the core and along the interface depend on the applied loads and the geometry of the sandwich plate, and are determined numerically.

3. SIMULATION OF CRACK GROWTH

We consider a sandwich double cantilever beam (DCB) specimen of length 152.4 mm (6 in) and width 25.4 mm (1 in) loaded by a concentrated load at a distance 25.4 mm (1 in) from its end (Fig. 1). The beam is made of aluminum

Table 1. Material Properties

Materials	t (mm)	E (GPa)	ν	\bar{E} (GPa)	G_{Incr} (Nmm/mm ²)	G_{Per} (Nmm/mm ²)
Al2024T3	1.00	62.30	0.33	69.95		
AralditeAV138M	0.30	4.700	-0.22	4.939		
Divinycell H60	25.40	0.056	0.26	0.059	0.28	0.10
Divinycell H80	25.40	0.080	0.29	0.087	0.45	0.22
Divinycell H100	25.40	0.100	0.25	0.107	0.78	0.30
Divinycell H250	25.40	0.280	0.30	0.308	1.55	1.00

2024 T3 facings of thickness 1 mm and a PVC foam (Divinycell H) core of thickness 25.4 mm (1 in). The core is bonded to the facings by of epoxy adhesive (Araldite AV 138M paste with HV998 hardener [22]) of thickness 0.3 mm. Four different PVC core materials, H60, H80, H100, and H 250, with densities 60, 80, 100 and 250 Kg/m³ were studied [23]. Material properties are given in Table 1. All Divinycell core materials are considered as linear elastic and isotropic. The specimen configuration follows that proposed by Prasad and Carlsson [10, 11], which is similar to the standard ASTM D5528-94a test [24]. An interfacial crack of length 51.1 mm is introduced between the core and the adhesive at the loaded end of the specimen. Propagation of the interfacial crack is studied under condition of plane strain.

Modeling and analysis is performed using a computer program developed by the Fracture Group of Cornell University under the commercial name FRANC 2D [25]. The initial meshing, the fracture toughness parameters (K_{Icr} , $G_{in,cr}(\gamma)$) and the initial crack configuration are first introduced. Then, as the crack propagates FRANC 2D removes automatically the affected portions of the mesh, places a new rosette of appropriate size around the new crack tip and performs local re-meshing semi-automatically. The elastic stress and displacement fields and the stress intensity factors are obtained, and the preferred direction of crack propagation is calculated based on the maximum circumferential stress criterion [16]. The crack tip is then moved to its new location by a user-specified increment.

The model of the sandwich DCB specimen is shown in Fig. (3). It is composed of seven topological regions. Each region is divided into regular and transition sub-regions. Sub-region boundaries are then subdivided into segments of appropriate number and proportions, and meshing is done automatically by boundary extrapolation, using Q8 and T6 elements for regular and transition sub-regions, respectively. The initial model contains 1501 elements (986 Q8 and 515

T6), of which 282 discretize the upper face, 114 the upper layer of adhesive, 97 the lower layer of adhesive, 97 the lower facing and 911 the core.

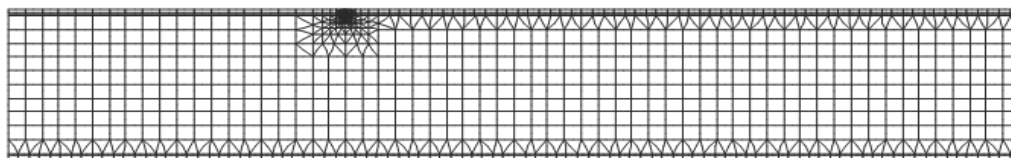
Fig. (4) shows the mesh part of the specimen with the applied concentrated load and the interfacial crack. The interfacial crack has an initial length of 25.4 mm and depth of 0.3 mm, and is introduced between the upper layer of adhesive and the core. It is surrounded by a two-layer octagonal rosette, which is surrounded by a local T6 transition mesh. The internal layer covers 30% of the rosette radius and is made of triangular square-root-singular elements (degenerate quarter-point Q8, [25]), whereas the external layer covers 70% of the radius and is made of trapezoidal Q8 elements. The ability of FRANC 2D to work with square-root-singular elements is of major importance since it can model the inverse square root singularity in the neighborhood of the crack tip.

The initial model is analyzed based on Eq. (3) (for $\beta = \varepsilon = 0$) to obtain the initial stress intensity factors (SIFs) by means of the displacement correlation method, which works correctly both for interfacial and core cracks. In the case of three-noded edges of square-root singular elements, the stress intensity factor is given by [26]:

$$\mathbf{K} = K_{II} \mathbf{e}_1 + K_I \mathbf{e}_2 = \frac{\sqrt{2\pi E}}{4\sqrt{l}} (4\Delta\mathbf{u}_{1/4} - \Delta\mathbf{u}_1) \quad (8)$$

where $\Delta\mathbf{u}$ is the vector of relative crack flank displacements. On the basis of the SIFs obtained, FRANC 2D identifies the three directions of propagation (along the interface, into the core, or into the adhesive) and computes the associated energy release rates. Then Eq. (7) is used to determine whether the crack will propagate in the facing, the adhesive or the core.

The PVC-foam core is porous and has very strong chemical affinity with the epoxy adhesive. Thus, the critical

**Fig. (3).** Initial meshing.

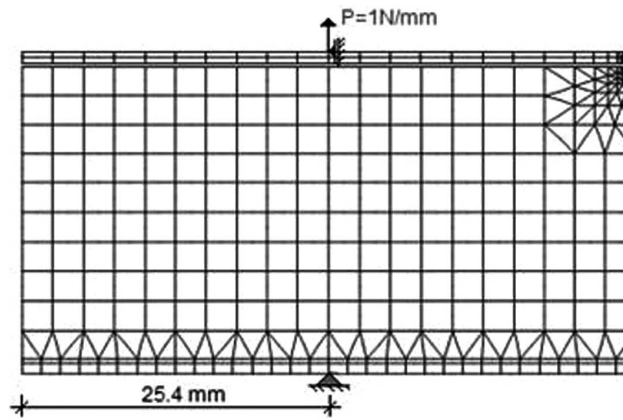


Fig. (4). Finite element discretization and loading.

interfacial energy release rate, $G_{int,cr}$, is expected to be greater than the that for crack propagation in the core, $G_{l,cr}$. In fact, experimental values reported in [27] suggest $G_{int,cr} \sim 2G_{l,cr}$ (Table 1), so that for any initial interfacial length, the crack kinks into the core. In view of these observations, we consider two sequences of configurations (trajectories) for each model:

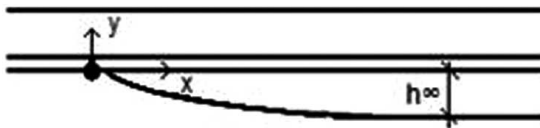


Fig. (5). Curved interfacial crack propagation in the core.

- a natural trajectory, where the crack kinks into the core (subsequent propagation according to the maximum circumferential stress criterion), and
- an artificial trajectory, where the crack is forced to stay on the interface, by introducing artificially low values for $G_{int,cr}$.

The natural trajectory near the kink is followed in very small crack increments, since it exhibits high curvature. In both cases the crack is simulated for values of the distance from the crack tip, x , up to 25.4 mm (1 in), where x is measured from the lower re-entrant corner as shown in Fig. (5). The results obtained for the artificial trajectory serve as reference values and a basis for comparisons.

4. NUMERICAL RESULTS AND DISCUSSION

For the prediction of the crack trajectory we use the interface toughness values for normal adhesion (Table 1). It is obtained that first the interfacial crack kinks into the core and then curves back toward the interface (Fig. 6). For intermediate values of the distance x from the crack tip ($3 \text{ mm} < x < 30 \text{ mm}$), we obtain the following results:

- the crack after a at a small depth h_{∞} becomes parallel to the interface (as shown in Fig. 5)

- $K_{I,int}$, $K_{II,int}$, and $K_{I,core}$ vary linearly with the distance x from the crack tip linear in x (Fig. 7), and
- G_{int} and G_{core} vary linearly with x and are almost independent of the core properties (Fig. 8).

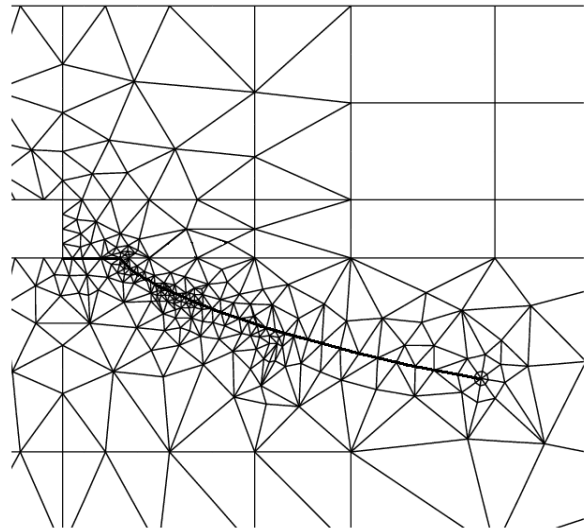


Fig. (6). Initial crack path trajectory.

Regarding the sub-interfacial crack propagation into the core we observe that the crack becomes parallel to the interface at a constant depth h_{∞} . An explanation of the constant value of h_{∞} and the linear variation of stress intensity factors with the distance from the crack tip x can be obtained by noting that the debonded part of the specimen (above the crack) can be considered as a thin cantilever beam ($l/d \sim 25$), elastically supported by the foam core, and subjected to a dominant bending moment varying linearly with x and to a relatively small (constant) shear force. Thus, the near-tip stress field is linearly proportional to x and, hence, the crack propagates in a self-similar manner parallel to the interface. The strain energy release rate can be determined by differentiating the work of the applied load with respect to the distance from the crack tip and is constant during crack propagation.

The core stiffness appears to be the main factor that influences the value of the asymptotic depth h_{∞} . Indeed, it can be obtained from Table 2 that the product $\bar{E}h_{\infty}$ is almost constant and equal to 60 N/mm for the three PVC foam materials H60, H80 and H250. For H100 it takes the value 70 N/mm. Thus, the depth h_{∞} is inversely proportional to the modulus of elasticity of the core material.

CONCLUSIONS

An investigation of the debonding of the facing from the core in sandwich structures with relatively soft brittle core materials (PVC foams) and stiff facings (aluminum) under a concentrated load pertaining to the standard “peel test” (ASTM D5528-94a) was undertaken. Under such conditions and for a critical applied load, debonding propagates along

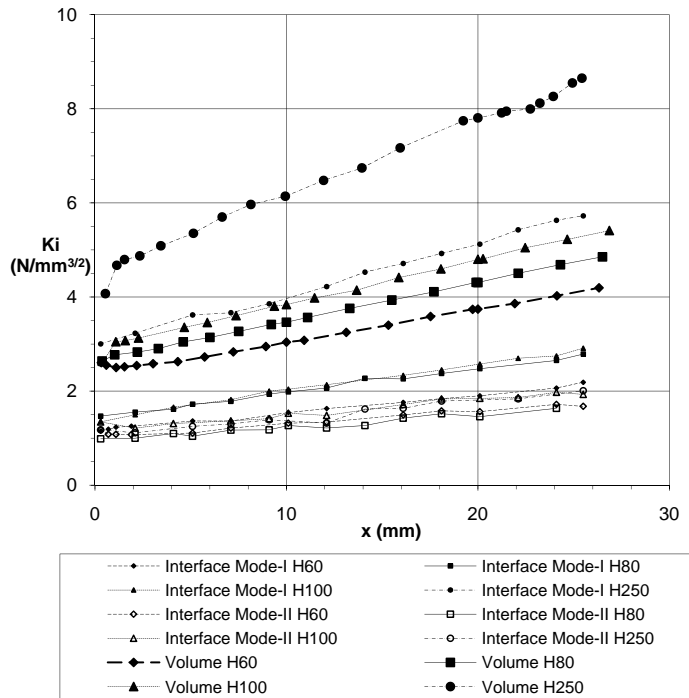


Fig. (7). Dependence of the SIFs on the distance from the crack tip.

Table 2. Values of Critical Distance h_{∞} and Strain Energy Release Rates

	\bar{E}	h_{∞}	$\bar{E}h_{\infty}$	$G_{core}(x) \approx \zeta_0 + \zeta_1 x + \zeta_2 x^2$			$\frac{G_{core}}{G_{int}} \Big _{3mm}$	$\frac{G_{core}}{G_{int}} \Big _{30mm}$
	(GPa)	(mm)	(N/mm)	$\zeta_0 * 10^2$	$\zeta_1 * 10^3$	$\zeta_2 * 10^5$		
H 60	0.059	1.01	59.6	9.4	5.4	7.7	2.3	2.3
H 80	0.087	0.70	60.9	8.0	5.1	8.1	2.3	2.3
H 100	0.107	0.65	69.6	8.0	5.1	8.1	2.5	2.4
H 250	0.308	0.20	61.6	6.7	4.8	8.7	2.0	2.0

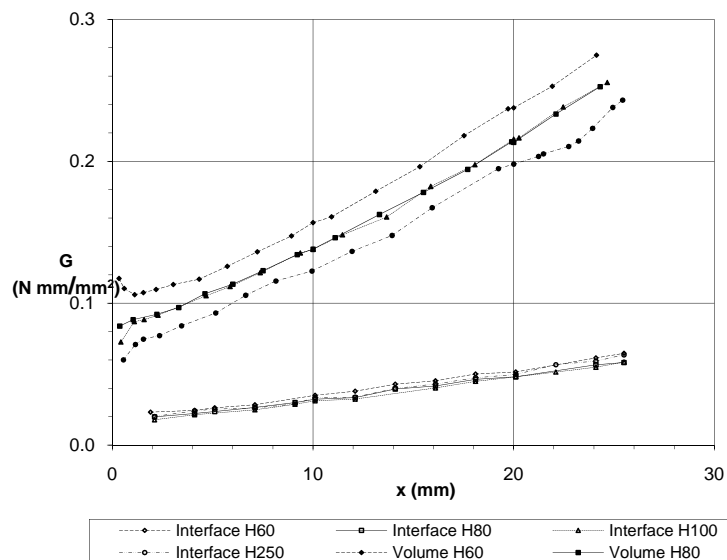


Fig. (8). Dependence of the energy release rates on the distance x from the crack tip.

the interface only when the adhesion between the interface and the core is weak. Otherwise, the crack kinks into the core and after a small initial curved path it propagates parallel to the interface at a depth h_{∞} . The value of h_{∞} is inversely proportional to the modulus of elasticity of the core. This behavior is independent of the core thickness, which is an order of magnitude larger than the thickness of the facing and the adhesive. Away from boundary effects (e.g., concentrated loads, beam supports, crack kinking, etc.) both stress intensity factors and strain energy release rate can be approximated as linear functions of the crack length.

REFERENTES

- [1] Gdoutos EE, Daniel IM, Wang K-A. Indentation failure in composite sandwich structures. *Exp Mech* 2002; 42: 426-31.
- [2] Daniel IM, Gdoutos EE, Wang K-A. Failure of composite sandwich beams. *Adv Comp Lett* 2002; 11: 49-57.
- [3] Daniel IM, Gdoutos EE, Wang K-A, Abot JL. Failure modes of composite sandwich beams. *Int J Damage Mech* 2002; 11: 309-34.
- [4] Abot JL, Daniel IM, Gdoutos EE. Failure mechanisms of composite sandwich beams under impact loading. In: *Proceeding of the 14th European Conference on Fracture*, Cracow, Neimitz A, Rokach IV, Kocanda D, Golos K, Eds. September 8-13, 2002; 2002.
- [5] Gdoutos EE, Daniel IM, Wang K-A. Compression facing wrinkling of composite sandwich structures. *Mech Mater* 2003; 35: 511-22.
- [6] Gdoutos EE. *Fracture mechanics criteria and applications*. Dordrecht: Kluwer Academic Publishers 1990.
- [7] Gdoutos EE. *Fracture mechanics – an introduction*. 2nd ed. New York: Springer 2005.
- [8] Zenkert D. Strength of sandwich structures with interface debondings. *Compos Struct* 1991; 17: 331-50.
- [9] Carlsson LA, Prasad S. Interfacial fracture of sandwich beams. *Eng Fract Mech* 1993; 44: 581-90.
- [10] Prasad S, Carlsson LA. Debonding and crack kinking in foam core sandwich beams – I: analysis of fracture specimens. *Eng Fract Mech* 1994; 47: 813-24.
- [11] Prasad S, Carlsson LA. Debonding and crack kinking in foam core sandwich beams – II: experimental investigation. *Eng Fract Mech* 1994; 47: 825-41.
- [12] Ratcliffe J, Cantwell WJ. Center notch flexure sandwich geometry for characterizing skin-core adhesion in thin-skinned sandwich structures. *J Reinforced Plastic Compos* 2001; 20: 945-70.
- [13] Østergaard RC, Sørensen BF, Brøndsted P. Measurement of interface fracture toughness of sandwich structures under mixed mode loadings. *J Sandwich Struct Mater* 2007; 9: 445-66.
- [14] Berggreen C, Simonsen BC, Borum KK. Experimental and numerical study of interface crack propagation in foam-cored sandwich beams. *J Comp Mater* 2007; 41: 493-520.
- [15] Grau DL, Qiu XS, Sankar BV. Relation between interfacial fracture toughness and mode-mixity in honeycomb core sandwich composites. *J Sandwich Struct Mater* 2006; 8: 187-203.
- [16] Erdogan F, Sih GC. On the crack extension in plates under plane loading and transverse shear. *J Bas Eng* 1963; 85: 519-27.
- [17] Hutchinson JW, Mear ME, Rice JR. Crack paralleling an interface between dissimilar materials. *J Appl Mech* 1987; 54: 828-32.
- [18] Rice JR. Elastic fracture mechanics concepts for interface cracks. *J Appl Mech* 1988; 55: 98-103.
- [19] He M-Y, Hutchinson JW. Kinking of a crack out of an interface. *J Appl Mech* 1989; 56: 270-8.
- [20] Zacharopoulos DA, Gdoutos EE, Bekiaris A. Crack kinking along a bimaterial interface. In *Proceedings of 1st Hellenic Conference on Composite Mater and Structure*. Xanthi, Greece, 1997.
- [21] Dundurs J. Edge-bonded dissimilar orthogonal elastic wedges under normal and shear loading. *J Appl Mech* 1969; 3: 650-2.
- [22] Arardite Technical manual for Adhesive AV 138M with Hardener HV 998
- [23] DIAB International AB, Divinycell Grade H Technical Manual 2003.
- [24] ASTM Standard D5528-94a. Standard test method for mode-I interlaminar fracture toughness of unidirectional fiber-reinforced polymer matrix composites. *ASTM Annual Book of ASTM Standard 15.03*, American Society for Testing and Materials 1999; pp. 283-292.
- [25] Ingraffea A, Wawrzynek P. User's guide for FRANC2D Version 3.1, 1993. Available at: <http://www.cfd.cornell.edu>
- [26] Weiler K. Edge-based data structures for solid modeling curved-surface environments. *IEEE Comput Graph Appl* 1985; 5: 21-40.
- [27] Shivakumar K, Chen H, Smith AS. An evaluation of data reduction methods for opening mode fracture toughness of sandwich panels. *J Sandwich Struct Mater* 2005; 7: 77-90.

Received: December 12, 2009

Revised: March 07, 2010

Accepted: April 06, 2010

© Gdoutos and Balopoulos; Licensee *Bentham Open*.

This is an open access article licensed under the terms of the Creative Commons Attribution Non-Commercial License (<http://creativecommons.org/licenses/by-nc/3.0/>) which permits unrestricted, non-commercial use, distribution and reproduction in any medium, provided the work is properly cited.